International Journal of Electrical, Electronic and Communication Sciences
ISSN: 2517-9438
Vol:6, No:12, 2012

# Algorithm of Measurement of Noise Signal Power in the Presence of Narrowband Interference

Alexey V. Klyuev, Valery P. Samarin, and Viktor F. Klyuev

***Abstract*****—**A power measurement algorithm of the input mix components of the noise signal and narrowband interference is considered using functional transformations of the input mix in the postdetection processing channel. The algorithm efficiency analysis has been carried out for different interference-to-signal ratio. Algorithm performance features have been explored by numerical experiment results.

***Keywords*****—**Noise signal; continuous narrowband interference; signal power; spectrum width; detection.

## I. Introduction

THIS paper presents a method of measurement of power of components of input mix of the noise signal and narrowband interference. The algorithm developed on the basis of this method, can be used, for example, in the structure of radiometer at radio-astronomical and other precision measurements of power of noise signals of a small level in the presence of narrowband interference with simultaneous measurement of its mean power [1]-[4], also the algorithm relevant for integration with GPS-type localization or power control for CDMA reception [5], [6]. Algorithm work based on measurement of total power of noise signal and narrowband interference, and also measurement of power of the low-frequency noise caused by interaction of noise signal and narrowband interference, arising after detection of input mix.

## II. Principle of Algorithm Work

In Fig. 1 the block diagram of the offered algorithm of measurement of power of noise signal and narrowband interference is presented.

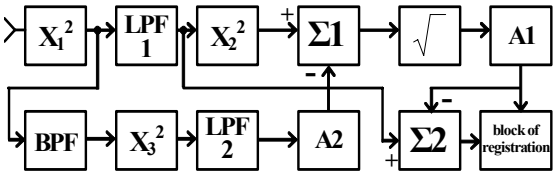


Fig. 1 Block diagram of the algorithm of measurement of power of noise signal and narrowband interference

In the input of the square-law device ($X_1^2$) the additive mix of the noise signal with spectrum $G_n(\omega)$ and narrowband interference with spectrum $G_i(\omega)$ from the output of high-frequency (HF) section of measuring system is present. The spectrum of noise signal $G_n(\omega)$ has width $\Pi_n$. The spectrum of narrowband interference $G_i(\omega)$ has width $\Pi_i$. The spectrum width $\Pi_n$ of noise signal is equal to width of HF section. In our case input process $u_{input}(t)$ contains narrowband interference $u_i(t)$ with the central frequency $(\omega_0+\Omega)$ and noise $u_n(t)$ with the central frequency $\omega_0$ (Fig. 2). Each of realizations of such noise can be presented in the form of quasi-harmonic process with envelope $U_n(t)$ and phase $\varphi_n(t)$, where $U_n(t)$ and $\varphi_n(t)$ random slowly varying functions of time [2]. Similarly, each of realizations of narrowband interference $u_i(t)$ can be presented in the form of quasi-harmonic fluctuations with envelope $U_i(t)$ and phase $\varphi_i(t)$, where $U_i(t)$ and $\varphi_i(t)$ are also random slowly varying functions of time. We assume that the spectrum width of narrowband interference is much less then the spectrum width of noise signal $\Pi_i << \Pi_n$.

Thus:

$$u_{input}(t)=u_i(t)+u_n(t)= \\ =U_i(t)\cos[(\omega_0+\Omega)t+\varphi_i(t)]+U_n(t)\cos[\omega_0 t+\varphi_n(t)] \quad (1)$$

Spectra of components in the input of the square-law device ($X_1^2$) are presented in Fig. 2.

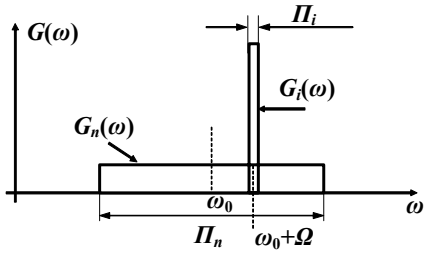


Fig. 2 Spectra of components of the additive mix of the noise signal and narrowband interference in the input of the square-law device ($X_1^2$)

A. V. Klyuev is with the Department of Bionics and Statistical Radiophysics, Lobachevsky State University of Nizhni Novgorod, Nizhni Novgorod, 603950 Russian Federation (phone: +7-831-465-6153; fax: +7-831-462-3260; e-mail: klyuev@rf.unn.ru).

V. P. Samarin is with the Department of machines and mechanisms, Nizhni Novgorod Military Institute of Engineering, Kstovo, 607650 Russian Federation (phone: +7-83145-30554; e-mail: samarin.vp@mail.ru).

V. F. Klyuev is with the Department of radio engineering, Lobachevsky State University of Nizhni Novgorod, Nizhni Novgorod, 603950 Russian Federation (phone: +7-831-465-6601; e-mail: klyuev@rf.unn.ru).

The voltage in the output of the first square-law device ($X_1^2$) contains a constant component and noise component, caused by noise signal, interference and interaction between noise signal and interference [2], [3]:

$$u_{square1}(t)= u_i^2(t)+u_n^2(t)+2\,u_i(t)u_n(t)= \\ =(1/2)[U_i^2(t)+U_n^2(t)+2U_i(t)U_n(t)\cos[\Omega t+\varphi_i(t)-\varphi_n(t)]]. \quad (2)$$

We can write expression for spectrum $G_{n\ output}(\omega)$ of process $u_n^2(t)$:

$$G_{n\,output} = \sigma_n^4\delta(\omega)+2\int_{-\infty}^{+\infty}G_n(\omega_1)G_n(\omega_1-\omega)d\omega_1 . \quad (3)$$

In relation (3) the first component describes spectrum $G_{nc} = \sigma_n^4\,\delta(\omega)$ of constant component, and the second - spectrum $G_{nfl}(\omega)$ of noise component. Here $\delta(\omega)$ - Dirac delta-function. The structure of subintegral expression of the second component in (3) shows, that $G_{nfl}(\omega)$ noticeably differs from zero only at $\omega \approx 0$ and $\omega \approx 2\omega_0$. Therefore spectrum $G_{nfl}(\omega)$ can be presented as the sum of spectra of low-frequency and high-frequency noise: $G_{nfl}(\omega) = G_{nlf}(\omega) + G_{nhf}(\omega)$, where $G_{nlf}(\omega)\approx G_{nfl}(\omega)$ at $\omega\approx 0$ and $G_{nhf}(\omega)\approx G_{nfl}(\omega)$ at $\omega\approx 2\omega_0$. The spectrum of low-frequency noise is presented in Fig. 3.

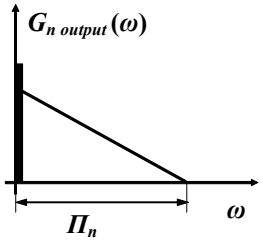


Fig. 3 Spectrum of low-frequency noise of process $u_n^2(t)$ in the output of the first square-law device

Using Gaussian approach, we can write expression for spectrum $G_{i\ output}(\omega)$ of process $u_i^2(t)$:

$$G_{i\,output} = \sigma_i^4\delta(\omega)+2\int_{-\infty}^{+\infty}G_i(\omega_1)G_i(\omega_1-\omega)d\omega_1 . \quad (4)$$

In relation (4) the first component describes spectrum $G_{ic} = \sigma_i^4\,\delta(\omega)$ of constant component, and the second - spectrum $G_{ifl}(\omega)$ of noise component. The structure of subintegral expression of the second component in (4) shows that $G_{ifl}(\omega)$ noticeably differs from zero only at $\omega\approx 0$ and $\omega \approx 2(\omega_0+\Omega)$. Therefore spectrum $G_{ifl}(\omega)$ can be presented as the sum of spectra of low-frequency and high-frequency noise: $G_{ifl}(\omega) = G_{ilf}(\omega) + G_{ihf}(\omega)$, where $G_{ilf}(\omega)\approx G_{ifl}(\omega)$ at $\omega \approx 0$ and $G_{ihf}(\omega)\approx G_{ifl}(\omega)$ at $\omega\approx 2(\omega_0+\Omega)$. The spectrum of low-frequency noise is presented in Fig. 4.

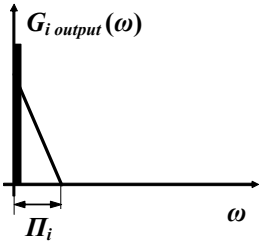


Fig. 4 Spectrum of low-frequency noise of process $u_i^2(t)$ in the output of the first square-law device

Relation for spectrum $G_{in\ output}(\omega)$ of $2u_i(t)u_n(t)$ is:

$$G_{in\,output} = 2\int_{-\infty}^{+\infty}G_i(\omega_1)G_n(\omega_1-\omega)d\omega_1 . \quad (5)$$

It is possible to present this spectrum as the sum of spectra of low-frequency and high-frequency noise: $G_{inf}(\omega) = G_{inlf}(\omega) + G_{inhf}(\omega)$. Low-frequency parts of spectrum at different values of offset $\Omega$ are presented in Fig. 5.

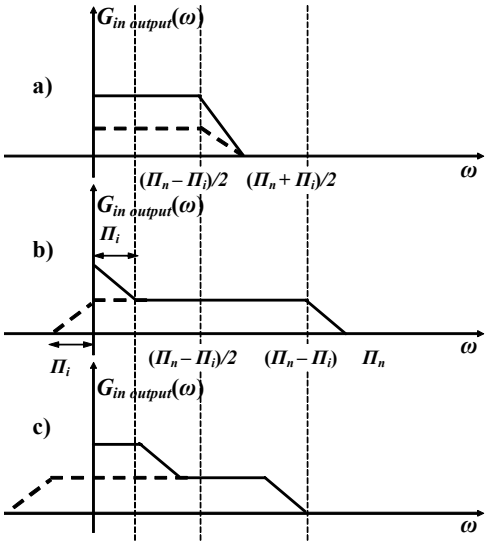


Fig. 5 Low-frequency parts of spectrum of process $2u_i(t)u_n(t)$ in the output of the first square-law device at different values of offset $\Omega$

In Fig. 5-a the case $\Omega$=0 is presented; in Fig. 5-b presented the case of the maximum offset $\Omega=(\Pi_n-\Pi_i)/2$; and in Fig. 5-c presented case of offset $0 < \Omega < (\Pi_n-\Pi_i)/2$.

Total spectrum $G(\omega)$ in the output of the first square-law device for a case $0 < \Omega < (\Pi_n-\Pi_i)/2$ is shown in Fig. 6.

In the output of the first low-pass filter (LPF 1) with band $\Pi_{LPF1}$, we have the mean value (constant component) proportional to the total power of noise signal $\sigma_n^2$ and narrowband interference $\sigma_i^2$:

$$u_{LPF1} = \sigma_i^2+\sigma_n^2+\mu. \quad (6)$$

In relation (6) $\mu$ shows, that the low-pass filter (LPF 1) cuts out a narrow band from a continuous part of a spectrum. However, this addition to a constant component is negligible

small.

The voltage from the output of the first low-pass filter (LPF 1) squared by square-law device ($X_2^2$):

$$u_{square2} = \sigma_i^4 + \sigma_n^4 + 2\sigma_i^2\sigma_n^2 + \mu_{square2}, \quad (7)$$

where $\mu_{square2}$ - result of transformation $\mu$ by the square-law device ($X_2^2$). In the adder ($\sum 1$) from the received voltage the output voltage from the second low-pass filter (LPF 2) is subtracted and the square root by the square-law device ($\sqrt{}$) is taken.

Generally, for optimum work of algorithm, lower $\omega_L$ and higher $\omega_H$ pass frequencies of the band-pass filter (BPF) must be $\omega_L \approx \Pi_i$ and $\omega_H \approx \Pi_i + \Pi_n$. It is necessary to exclude component proportional to a square of narrowband interference voltage $(1/2)U_i^2(t)$, see (2). However, in real conditions the spectrum width of the narrowband interference $\Pi_i$ is unknown. We assume that the width spectrum of the narrowband interference is much less than the width spectrum of the noise signal $\Pi_i << \Pi_n$. Therefore, the frequency $\omega_L$ must be chosen enough small. In case of such specified characteristics of the band-pass filter (BPF) on the input of the third square-law device ($X_3^2$) there are fluctuations caused by noise signal and interaction between noise signal and interference only.

$$u_{BPF}(t) = (1/2)U_n^2(t) + U_n(t)U_i(t)\cos[\Omega t + \varphi_i(t) - \varphi_n(t)]] \quad (8)$$

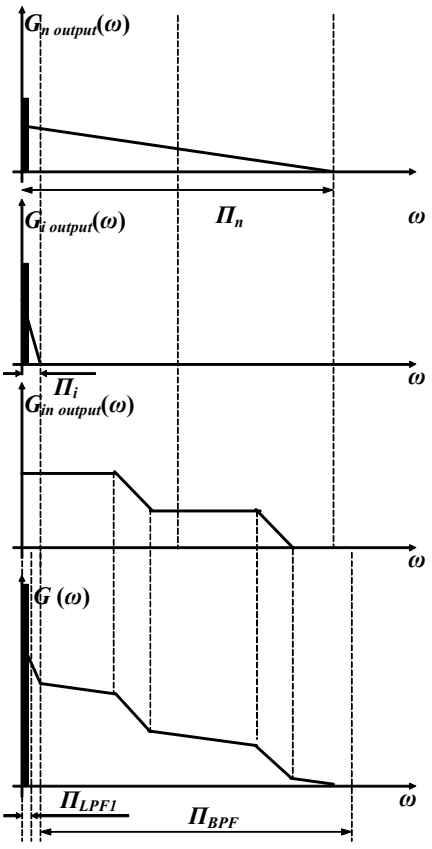


Fig. 6 Low-frequency part of total spectrum $G(\omega)$ on the output of the first square-law device for the case $0 < \Omega < (\Pi_n - \Pi_i)/2$

In spectral domain this illustrates Fig. 6.

Therefore, the constant component in the output of the third square-law device ($X_3^2$), extracted by the second low-pass filter (LPF 2), is proportional to the power of these fluctuations only:

$$u_{square3} = \sigma_n^4 + 2\sigma_i^2\sigma_n^2. \quad (9)$$

Separate measurement of $\sigma_n^2$ and $\sigma_i^2$ is reached as follows. The transfer factor of attenuator (A2) must be chosen so that at switched on source of noise signal and switched off source of interference the voltage on the output of the first adder ($\sum 1$) equal zero. Attenuator (A1) adjusted so that the voltage in the output of the second adder ($\sum 2$) does not depend on a source of interference. As a result the voltage in the first input of the block of registration depends on the power of noise signal only, and in the second - on the power of interference only, and separate measurement of power of noise signal and power of interference is reached.

## III. Simulation Results

In this section, we give simulation results for the power measurement algorithm of the input mix components of the noise signal and narrowband interference, based on the method described in the previous sections.

The offered algorithm is based on modelling of work of typical elements of a low-frequency section of measuring system [2]-[4]: the square-law device, the first low-pass filter, the adder, the band-pass filter, the additional square-law device, the second low-pass filter and the block of registration. It is realized in program environment LabVIEW 7.0 [7]. The narrowband interference was modelled by a sine wave signal of constant amplitude and frequency. The noise signal from the output of a high-frequency section was modelled by white Gaussian noise from standard library of LabVIEW 7.0 passed through the band-pass filter. On the input we have the additive mix of a noise signal and a sine wave interference. We vary amplitude of a sine wave interference, and dispersion of noise in the input. Relative offset $(\omega_0 + \Omega)/\omega_0 = 1.125$. From the principle of work of the method follows, that work of algorithm does not depend on frequency of a sine wave interference.

Dependence of error of measurement of average power of noise signal $\varepsilon_n$ and dependence of error of measurement of average power of sine wave interference $\varepsilon_s$ on the ratio interference/(noise signal) $\rho$ (see Fig.7) has been investigated.

Here $\varepsilon_n$ – relative error of measurement of average power of noise signal $\varepsilon_n = |(\sigma_n^2 - \sigma_{no}^2)/\sigma_n^2|$, where $\sigma_n^2$ – average power of input noise signal, $\sigma_{no}^2$ – estimation of average power of noise signal in the output; $\rho = \sigma_s^2/\sigma_n^2$ – the ratio of the average power of sine wave interference in the input to the average power of noise signal in the input.

Here $\varepsilon_s$ – relative error of measurement of average power of sine wave interference $\varepsilon_s = |(\sigma_s^2 - \sigma_{so}^2)/\sigma_s^2|$, where $\sigma_{so}^2$ – estimation of average power of sine wave interference in the output.

Besides, in Fig. 7 shown $\varepsilon$ - a relative error of measurement

of average power of noise signal in the presence of sine wave interference without any additional processing. $\varepsilon$ is defined by relation $\varepsilon=|(\sigma_n^2 - \sigma^2)/\sigma_n^2|$, where $\sigma^2$ an estimation of average power of mix.

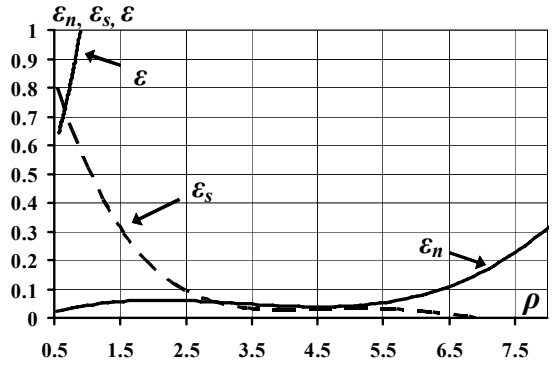


Fig. 7 Dependence $\varepsilon_n$, $\varepsilon_s$ and $\varepsilon$ on $\rho$

For convenience of the analysis of the obtained dependences, relative error of measurement of average power of noise signal $\varepsilon_n$, relative error of measurement of average power of sine wave interference $\varepsilon_s$ and $\varepsilon$ are shown in one figure – Fig. 7.

From Fig. 7 it is seen, that down to $\rho \leq 6$ relative error of measurement of average power of noise signal $\varepsilon_n$ not exceed 5 %.

As it seen from Fig. 7, if we measure power of noise signal in the presence of sine wave interference without offered method, error of measurement of average power of noise signal (curve $\varepsilon$ in Fig. 7) many times over exceeds corresponding error in case of using the method (curve $\varepsilon_n$ in Fig. 7).

Through analysis of algorithm work, it is shown that when the ratio interference/(noise signal) increase, the error of measurement of average power of noise signal increase, and the error of measurement of average power of sine wave interference $\varepsilon_s$ decrease.

## IV. Conclusion

In this paper, we have presented the power measurement algorithm of the input mix components of the noise signal and narrowband interference. Results are confirmed by numerical experiments. It is shown, that with increasing of the ratio interference/(noise signal) the error of measurement of the average power of noise signal increases, however even at $\rho \approx 6$ does not exceed 5 %. Application of the considered algorithm allows receiving more than tenfold increase of accuracy of measurement of average power of noise signal. Thus, at $\rho \geq 3$ error of measurement of average power of interference less than 5 %. Results of work have practical value for designing real systems of measurement of power of noise signals in the presence of narrowband interferences.

## Acknowledgment

The authors thank Prof. Dr., Dean of Radiophysics Faculty of Lobachevsky State University of Nizhni Novgorod Arkady V. Yakimov for important remarks and useful advices on the work.

The research was carried out in Nizhni Novgorod State University in frames of Priority National Project “Education”. The investigations were supported by Program: “Scientific and scientific-pedagogical personnel of innovative Russia” for 2009–2013 years (State–contract No. P2606).

## References

[1] Patent 1541537 USSR. Measuring instrument of power of noise signal, V.P. Samarin, V.F. Klyuev, M.Ya. Ovcharov, M.M. Leifer, Declared 21.06.88; published 8.10.89, № 5.

[2] V.F. Klyuev, V.P. Samarin, A.V. Klyuev, “Estimation of efficiency of algorithm of measurement of power of noise on the background of narrow-band interference.” *Information-measuring and Control Systems,* vol. 10, no 6, pp.72-75, 2012.

[3] V.F. Klyuev, V.P. Samarin, A.V. Klyuev, “Algorithm of measurement of power of noise on the background of irregular pulse interferences.” *Information-measuring and Control Systems,* vol. 10, no 1, pp.76-79, 2012.

[4] V.I. Vladimirov, A.A. Bubenshikov, S.V. Sidenko, “Simultaneous measurement of power of the signal and power of the noise in passband of the main channel.” *Information-measuring and Control Systems*, vol. 10, no 7, pp.67-72, 2012.

[5] S. W. Kim and A.J. Goldsmith, “Truncated Power Control in Code-Division Multiple-Access Communications,” *IEEE Trans. On Vehicular Technology*, vol. 49, no. 3, pp. 965–972, May 2000.

[6] S. W. Kim and A.J. Goldsmith, “Decentralized Dynamic Power Control for Cellular CDMA Systems,” *IEEE Trans. On Wireless Communications*, vol. 2, no. 3, pp. 549–559, May 2003.

[7] B. Paton, LabVIEW: Analog and digital electronics, National Instruments, 2002.